Quantum Electronics **39** (12) 1175 – 1181 (2009)

OPTICS OF NANOSTRUCTURES

PACS numbers: 42.55.Ks; 33.50.–j; 82.20.–w
DOI: 10.1070/QE2009v039n12ABEH014143

Controlling interface reflectance by a monolayer of nanoparticles

A.S. Shalin, S.G. Moiseev

***Abstract*. This work examines reflection of a light wave from the surface of a semi-infinite medium covered with an ordered monolayer of spherical nanoparticles. We derive analytical expressions for the electric fields within and outside such structures with allowance for the electrodynamic interaction of the nanoparticles with one another and with the substrate. It is shown that such metalayers may raise or reduce the reflection coefficient relative to Fresnel reflection from an uncoated substrate surface. Constructive and destructive interference conditions are examined. We derive and analyse a zero-reflection condition in the form of a relationship between the parameters of the monolayer and medium.**

Keywords: *metamaterial, monolayer of nanoparticles, light scattering by small particles.*

1. Introduction

Much attention has recently been paid to the optical properties of artificially structured materials containing various nanoscale objects embedded in a matrix, which are referred to as metamaterials [1 – 4]. The interest in metamaterials is generated by the possibility of observing a number of unusual effects related to their composite structure and the specifics of light scattering by nanoparticles. Indeed, varying the geometric and material parameters of a system, one can obtain, e.g., media with a giant, extremely small or negative refractive index [1, 5, 6] or with a real part of their refractive index close to unity [7].

A surface monolayer of spherical clusters was described theoretically by directly solving Maxwell's equations in spherical coordinates [8, 9]. Although the solution obtained by Mie [10] refers to diffraction from a single sphere, it can be generalised to any number of interacting particles using 3*j* symbols and Clebsch – Gordan coefficients, which allow one to take into account multiple coherent light scattering by nanoclusters in the structures in question [8]. This approach is however not always appropriate. Indeed, as shown earlier [8, 9, 11, 12] the interaction between particles is long-range and requires taking into account a rather large number of elements that influence each other. The problem can thus be treated in this approach only numerically, which requires a long computation time. Similar difficulties are encountered in other methods that directly solve Maxwell's equations, such as the finite element method (FEM) [13, 14], finite-difference time-domain (FDTD) method [15, 16], and coupled dipole method (CDM) [17]. Moreover, taking into account the interaction between a layer of nanoparticles and the substrate [9, 14, 17] adds considerable complexity to the computation process or requires a number of approximations, e.g., averaging of the refractive indices of the substrate and environment [18], which can be done by different procedures, or the introduction of an imaginary nanostructured layer, a reflection of the real layer [9].

A recently proposed theoretical approach [4, 11, 19] allows one to find a relatively simple analytical solution to the problem of light scattering by a system of nanoclusters in the long-wavelength approximation. The theory relies on an integral-equation formalism [8, 20], does not require Maxwell boundary conditions for evaluating the interaction parameters of nanoparticles in the layer and, as will be shown below, makes it possible to directly take into account the mutual polarisation of the medium and nanostructured layer. Note that the ability to find an analytical solution is essential for inverse optical problems, where the resultant optical properties are given *a priori*, whereas the underlying geometric and material parameters of the system are unknown. In this context, we propose using the above-mentioned integral-equation method and refining the results by electrodynamic finite element simulation in the COMSOL Multiphysics environment [21].

This work focuses on the interference interaction of an ordered monolayer of spherical nanoparticles with the substrate. The expressions obtained for the fields within and outside the system are used to examine the conditions under which its reflectance decreases or increases. We derive and analyse the condition for complete elimination of reflection from a medium (zero-reflection condition), which determines the geometric and material parameters of the nanoparticle monolayer necessary for suppressing the reflection from the substrate, and demonstrate that zero reflection is possible in a wide wavelength range.

A.S. Shalin V.A. Kotel'nikov Institute of Radio Engineering and Electronics (Ulyanovsk Branch), Russian Academy of Sciences, ul. Goncharova 48/2, 432011 Ulyanovsk, Russia; Ulyanovsk State University, ul. L'va Tolstogo 42, 432700 Ulyanovsk, Russia; e-mail: shalin_a@rambler.ru;
S.G. Moiseev V.A. Kotel'nikov Institute of Radio Engineering and Electronics (Ulyanovsk Branch), Russian Academy of Sciences, ul. Goncharova 48/2, 432011 Ulyanovsk, Russia; Ulyanovsk State Technical University, ul. Severnyi Venets 32, 432027 Ulyanovsk, Russia; e-mail: serg-moiseev@yandex.ru

Received 27 March 2009; revision received 7 August 2009
Kvantovaya Elektronika **39** (12) 1175 – 1181 (2009)
Translated by O.M. Tsarev

2. Constitutive equations

Figure 1 schematically shows a system comprising a layer of spherical nanoparticles and a substrate. The layer and substrate are infinite in the xy plane. To assess the electromagnetic response of the system, we use the integral-equation formalism [4, 8, 11, 12] that was applied earlier to study a variety of nanostructured arrays. Here we restrict ourselves to a linear approximation: the polarisations of the medium and particles are linear functions of field strength.

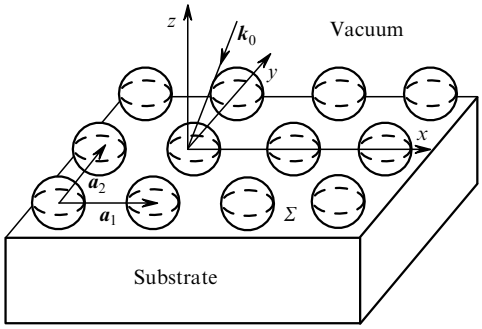

Figure 1. Geometry of the system. A wave with wave vector $\boldsymbol{k}_0$ is incident from vacuum on a surface, Σ, covered with an ordered layer of nanoparticles.

In this approach, the field at each point of space can be written in the form

$$\boldsymbol{E}(\boldsymbol{r},t)=\boldsymbol{E}_I(\boldsymbol{r},t)+\int_V \mathrm{rotrot}\,\frac{\boldsymbol{P}(\boldsymbol{r}',t-R/c)}{R}\,\mathrm{d}V'$$

$$+\frac{3}{4\pi}\sum_{j=1}^{N}\int_{V_j}\mathrm{rotrot}\,\frac{\varepsilon_j(\boldsymbol{r}_j')-1}{\varepsilon_j(\boldsymbol{r}_j')+2}\,\frac{\boldsymbol{E}'_{j\mathrm{eff}}(\boldsymbol{r}_j',t-R_j'/c)}{R_j'}\,\mathrm{d}V_j', \quad (1)$$

where $\boldsymbol{E}_I(\boldsymbol{r},t)=\boldsymbol{E}_{0I}\exp(\mathrm{i}\boldsymbol{k}_0\boldsymbol{r}-\mathrm{i}\omega t)$ is the wave at a point of observation with radius vector $\boldsymbol{r}$; the first integral represents the response of the substrate, whose polarisation $\boldsymbol{P}$ is proportional to the amplitude of the incident field; $R=|\boldsymbol{r}-\boldsymbol{r}'|$ is the distance from an integration point (radius vector $\boldsymbol{r}'$) in the medium to the point of observation; V is the volume of the medium; c is the speed of light in vacuum; and $(t-R/c)$ represents the time delay of the corresponding quantity. The second integral (more precisely, the sum of integrals) represents the field of the layer of N spherical nanoparticles interacting with it, which have a complex relative dielectric permittivity $\varepsilon_j(\boldsymbol{r})$ and volume $R_j=|\boldsymbol{r}-\boldsymbol{r}_j'|$; and $\boldsymbol{r}_j'$ is the radius vector of an integration point inside the jth nanoparticle. The effective field $\boldsymbol{E}'_{j\mathrm{eff}}$ in (1) differs from the incident plane wave $\boldsymbol{E}_I$ and has the form of a wave acting on each point in the jth nanoparticle, with allowance for the fields re-emitted by the nanoparticles and substrate. As shown earlier [20, 22], $\boldsymbol{E}'_{j\mathrm{eff}}$ comprises two contributions: external, due to the environment (the other particles of the monolayer and the substrate), and internal, which determines the interatomic interaction in the nanoparticle and the permittivity of the medium. Taking into account the internal field leads to separation of Eqn (1) into local and nonlocal parts, as described in detail elsewhere [20]. The former part reduces to the Lorentz–Lorenz formula, which relates the permittivity of a particle to the polarisability and concentration of its constituent atoms. The boundary problem is thus reduced to solving nonlocal equations, namely, to finding the fields $\boldsymbol{E}_{j\mathrm{eff}}$ that act on the nanoparticles from the environment.

For simplicity, consider a layer of identical homogeneous nanoclusters [$\varepsilon=\varepsilon_j$, $a=a_j$ ($j=1,\ldots,N$)] using the long-wavelength approximation, which can be represented by the conditions

$$k_0a,\,k_0a\mathrm{Re}n,\,k_0a\mathrm{Im}n\ll 1, \quad (2)$$

where k_0 is the wave vector of the incident wave, and a and $n=\sqrt{\varepsilon}$ are the radius and refractive index of the spherical clusters, respectively. With these conditions met, $\boldsymbol{E}_I$ and $\boldsymbol{E}_{j\mathrm{eff}}$ can be considered constant throughout a given cluster and equal to those in its centre.

Placing the point of observation and the origin in the centre of the ith particle, we write the nonlocal part of Eqn (1) in the form

$$\boldsymbol{E}_{i\mathrm{eff}}=\boldsymbol{E}_I(0,t)+\frac{3}{4\pi}\,\frac{\varepsilon-1}{\varepsilon+2}$$

$$\times\sum_{j=1,\,j\neq i}^{N}\int_{V_j}\mathrm{rotrot}\,\frac{\boldsymbol{E}_{j\mathrm{eff}}(\boldsymbol{r}_j',t-|\boldsymbol{r}_j'|/c)}{|\boldsymbol{r}_j'|}\,\mathrm{d}V_j'+(\hat{G}\boldsymbol{E}_{\mathrm{m}})_{(t-|\boldsymbol{\Delta}|/c)}. \quad (3)$$

The second term in the right-hand side of Eqn (3) represents the superposition of the fields produced by the nanoparticles in the centre of the ith particle. The third term represents the total field (with allowance for the contribution from the monolayer) reflected from the substrate surface, where $\hat{G}$ is the reflection coefficient; $\boldsymbol{E}_{\mathrm{m}}$ is the effective field incident on the substrate; and $t-|\boldsymbol{\Delta}|/c$ is the time delay by $|\boldsymbol{\Delta}|/c$, equal to the time it takes the wave to travel from the plane defined by the centres of the nanoparticles to the substrate surface, with $\boldsymbol{\Delta}=(0,0,-a)$. Taking into account the self-polarisation of the layer through the reflection of its field from the substrate surface is of key importance because neglecting this effect leads to considerable deviations from the exact solution. $\boldsymbol{E}_{\mathrm{m}}$ can be found from the nonlocal part of Eqn (1), by writing it for a point of observation on the substrate surface:

$$\boldsymbol{E}_{\mathrm{m}}=\boldsymbol{E}_I(\boldsymbol{\Delta},t)+\frac{3}{4\pi}\,\frac{\varepsilon-1}{\varepsilon+2}$$

$$\times\sum_{j=1}^{N}\int_{V_j}\mathrm{rotrot}\,\frac{\boldsymbol{E}_{j\mathrm{eff}}(\boldsymbol{r}_j',t-|\boldsymbol{\Delta}-\boldsymbol{r}_j'|/c)}{|\boldsymbol{\Delta}-\boldsymbol{r}_j'|}\,\mathrm{d}V_j'. \quad (4)$$

Equations (3) and (4) constitute a self-consistent system of integral equations, whose solution is the effective electric field in the monolayer. Unfortunately, the reflection coefficient $\hat{G}$ is rather difficult to calculate in general form [23]. In particular, the standard procedure based on the extinction theorem in integral form [20] cannot be used to perform the integration over the medium in (1) because the field produced by the nanoparticles in the surface layer of the substrate is inhomogeneous [9]. The solution can then be found using the above-mentioned coupled dipole method, which requires purely computational means. On the other

hand, as we showed previously [19] the reflection coefficient $\hat{G}$ of an inhomogeneous field can be approximated by a tensor constructed from the Fresnel reflection coefficients of a plane wave. In the optical region, this approximation is applicable when the characteristic values of the geometric parameters of the metalayer (lattice period and particle size) do not exceed a few tens of nanometres at a moderate absorption coefficient of the particles, which corresponds to conditions (2). The $\hat{G}$ tensor then has the form

$$G = \begin{pmatrix} r_\perp \sin^2\varphi - r_\parallel \cos^2\varphi & -(r_\perp + r_\parallel)\sin\varphi\cos\varphi & 0 \\ -(r_\perp + r_\parallel)\sin\varphi\cos\varphi & r_\perp \cos^2\varphi - r_\parallel \sin^2\varphi & 0 \\ 0 & 0 & r_\parallel \end{pmatrix},$$

where $r_\perp$ and $r_\parallel$ are the Fresnel reflection coefficients for the electric vector components normal and parallel to the plane of incidence [20] and φ is the angle between the plane of incidence and the x axis.

3. Optical fields in the nanostructured layer

Consider the field produced by the jth nanoparticle in vacuum at a point of observation with radius vector $\boldsymbol{R}$ outside the nanoparticle. In the long-wavelength approximation, the integrl representing the field strength in (1) can be calculated easily by the Ewald–Oseen method [20], as done in previous studies [11, 12, 24]. As a result, we obtain the relation

$$\boldsymbol{E}_{j\,\mathrm{sca}}(\boldsymbol{R}) = \alpha_p \hat{f}_j(R)\boldsymbol{E}_{j\,\mathrm{eff}} \tag{5}$$

($\alpha_p = a^3(\varepsilon - 1)/(\varepsilon + 2)$), where the $\hat{f}_j(R)$ tensor has the following components for the external-field polarisations parallel and normal to $\boldsymbol{R}$:

$$\begin{aligned} f_j^{\mathrm{p}}(R) &= \exp(\mathrm{i}k_0 R)\left(\frac{2}{R^3} - \frac{2\mathrm{i}k_0}{R^2}\right), \\ f_j^{\mathrm{s}}(R) &= \exp(\mathrm{i}k_0 R)\left(-\frac{1}{R^3} + \frac{\mathrm{i}k_0}{R^2} + \frac{k_0^2}{R}\right). \end{aligned} \tag{6}$$

According to Eqns (5) and (6), the field scattered by a nanoparticle strictly corresponds to that created by a dipole of polarisability α_p located in the centre of the particle [20, 22]. Clearly, if the particle is surrounded not by vacuum, the permittivity ε in (5) is relative rather than absolute.

Let us use the principle of parallel translational symmetry [25, 26], according to which an electric field (an external wave or the wave reflected from the substrate surface) incident on a layer of nanoparticles meets the condition

$$\boldsymbol{E}_{\mathrm{inc}}(\boldsymbol{r}_j) = \boldsymbol{E}_{\mathrm{inc}}(0)\exp(\mathrm{i}\boldsymbol{q}\boldsymbol{r}_j). \tag{7}$$

Here, $\boldsymbol{r}_j$ is the radius vector of the centre of the jth nanoparticle, and the components of the $\boldsymbol{q}$ vector are $(q_x, q_y, 0)$, where $q_x = k_{0x} = -k_0 \sin\theta_I \cos\varphi$ and $q_y = k_{0y} = -k_0 \sin\theta_I \sin\varphi$ (θ_I is the angle of incidence). Therefore, since all the clusters are identical, the field amplitudes are $\boldsymbol{E}_{j\,\mathrm{eff}} = \boldsymbol{E}_{i\,\mathrm{eff}} = \boldsymbol{E}_{\mathrm{eff}}$ and the phase shift is given by (7). With Eqns (5)–(7), the integrals in (3) and (4) can be converted to lattice sums:

$$\begin{aligned} &\frac{3}{4\pi}\frac{\varepsilon - 1}{\varepsilon + 2}\sum_{j=1}^{N}\int_{V_j} \mathrm{rotrot}\,\frac{\boldsymbol{E}_{\mathrm{eff}}(\boldsymbol{r}_j', t - R_j'/c)}{R_j'}\,\mathrm{d}V_j' \\ &\quad = \alpha_p \boldsymbol{E}_{\mathrm{eff}} \sum_{j=1}^{N} \hat{f}_j(|\boldsymbol{r} - \boldsymbol{r}_j|)\exp(\mathrm{i}\boldsymbol{q}\boldsymbol{r}_j). \end{aligned} \tag{8}$$

Therefore, the system of integral equations (3) and (4) reduces to the following linear algebraic equation for the field acting on a cluster:

$$\begin{aligned} \boldsymbol{E}_{\mathrm{eff}} &= \boldsymbol{E}_I(0) + \alpha_p \boldsymbol{E}_{\mathrm{eff}} \hat{A}_p \\ &\quad + \hat{G}\left[\boldsymbol{E}_I(0)\exp(2\mathrm{i}\boldsymbol{k}_0\boldsymbol{\Delta}) + \left(\alpha_p \boldsymbol{E}_{\mathrm{eff}} \hat{C}_p^-(2\boldsymbol{\Delta})\right)\right], \end{aligned} \tag{9}$$

where the term in square brackets is equal to $(\boldsymbol{E}_{\mathrm{m}})_{(t-|\boldsymbol{\Delta}|/c)}$ given that the wave reflected from the substrate lags the wave incident on the layer both in the path from the plane defined by the centres of the nanoparticles to the substrate surface and after the reflection, in the path from the substrate surface to that plane. In (9), we use the following designations:

$$\hat{A}_p = \sum_{j=1,\, j\neq i}^{N} \hat{f}_j(|\boldsymbol{r}_j|)\exp(\mathrm{i}\boldsymbol{q}\boldsymbol{r}_j), \tag{10}$$

is the lattice sum determining the field produced at the ith particle by the other particles in the layer and

$$\hat{C}_p^-(2\boldsymbol{\Delta}) = \left(\sum_{j=1}^{N} \hat{f}_j(|\boldsymbol{\Delta} - \boldsymbol{r}_j|)\exp(\mathrm{i}\boldsymbol{q}\boldsymbol{r}_j)\right)_{(t-|\boldsymbol{\Delta}|/c)} \tag{11}$$

is the lattice sum describing the field emitted by the layer towards the substrate (the superscript '$-$' denotes that the wave propagates in the negative direction relative to the z axis). The calculated lattice sums of the form (10) and (11) are given in the Appendix.

Solving Eqn (9) for the effective field acting on a nanoparticle in the monolayer, we obtain

$$\boldsymbol{E}_{\mathrm{eff}} = \frac{1 + \hat{G}\exp(2\mathrm{i}\boldsymbol{k}_0\boldsymbol{\Delta})}{1 - \alpha_p \hat{A}_p - \hat{G}\left(\alpha_p \hat{C}_p^-(2\boldsymbol{\Delta})\right)}\,\boldsymbol{E}_I(0). \tag{12}$$

The effective-polarisability approach allows one to deal with the external field strength without considering the parameters of the structure. From the relation

$$\boldsymbol{d}_p = \alpha_p \boldsymbol{E}_{\mathrm{eff}} = \hat{\alpha}_{p\,\mathrm{eff}} \boldsymbol{E}_I, \tag{13}$$

where $\boldsymbol{d}_p$ is the dipole moment of a nanocluster, we obtain the following formula for the effective polarisability of the nanoparticle:

$$\hat{\alpha}_{p\,\mathrm{eff}} = \alpha_p \frac{1 + \hat{G}\exp(2\mathrm{i}\boldsymbol{k}_0\boldsymbol{\Delta})}{1 - \alpha_p \hat{A}_p - \hat{G}\left(\alpha_p \hat{C}_p^-(2\boldsymbol{\Delta})\right)}. \tag{14}$$

4. Reflected wave field in the wave zone. Effect of a monolayer of particles on reflectance

At a point of observation with radius vector $\boldsymbol{p}$, the wave reflected from a monolayer–substrate system has the form

$$\begin{aligned} \boldsymbol{E}_{\mathrm{refl}}(\boldsymbol{p}) &= \left\{\hat{G}\exp\left[\mathrm{i}\boldsymbol{k}_0\boldsymbol{\Delta} + \mathrm{i}\boldsymbol{k}_{0\,\mathrm{refl}}(-\boldsymbol{\Delta} + \boldsymbol{p})\right]\right. \\ &\quad \left. + \hat{\alpha}_{p\,\mathrm{eff}}\left[\hat{G}\hat{C}_p^-(2\boldsymbol{\Delta} - \boldsymbol{p}) + \hat{C}_p^+(\boldsymbol{p})\right]\right\}\boldsymbol{E}_I, \end{aligned} \tag{15}$$

where the use of $-\boldsymbol{p}$ in $\hat{C}_p^-(2\boldsymbol{\Delta}-\boldsymbol{p})$ allows us to avoid dividing the wave path into two parts (in the z direction from the layer to the substrate surface and then in the opposite direction from the substrate to point $\boldsymbol{p}$) and to replace it with the total distance plotted in the z direction, and $\boldsymbol{k}_{0\,\mathrm{refl}} = (k_{0x}, k_{0y}, -k_{0z})$ is the wave vector of the reflected wave.

It follows from (15) that the reflected wave amplitude is the sum of three quantities. One of them, the first term in (15), represents Fresnel reflection from a flat substrate surface with no nanoparticles. The other two terms are due to the polarisation of the nanospheres, which interact electrodynamically with one another and with the substrate: $\alpha_{p\,\mathrm{eff}}\hat{C}_p^+(\boldsymbol{p})\boldsymbol{E}_I$ represents the emission from the monolayer in the reflected wave direction ($+z$ direction) and $\alpha_{p\,\mathrm{eff}}\hat{G}\times\hat{C}_p^-(2\boldsymbol{\Delta}-\boldsymbol{p})\boldsymbol{E}_I$ represents the emission from the monolayer to the substrate and that reflected from its surface. Since the phase factors of these terms depend significantly on the geometry and material parameters of the monolayer substrate system, interference of the corresponding waves at the point of observation may raise or reduce the reflection coefficient relative to the Fresnel coefficient.

From the data in Fig. 2, obtained by exact electrodynamic finite element computations [21], it is seen that the interfacial monolayer leads to light wave energy redistribution, characteristic of optical interference effects: a decrease in reflectance is always accompanied by an increase in the fraction of energy transmitted to the substrate, and vice versa. In transparent media, interference may be destructive only when $(n-n_1)(n_2-n_1)>0$, where n_1 and n_2 are the absolute refractive indices of two adjacent semi-infinite media. The relationship between the optical density of spherical particles and that of their environment determines the sign of the polarisability of the particles, α_p, and hence the phase shift of the waves generated by the monolayer of the particles. Thus, a change in the sign of $(n-n_1)$ leads to a change in the nature of the interference of the waves reflected from the entire structure, as evidenced by comparison of the data in Figs 2a and 2b with those in Fig. 2c.

Thus, the nature of interference of the waves reflected from the layer and substrate strongly depends on the relationship between the optical constants of the environment and substrate and the parameters of the monolayer, which allows the resultant reflectance to be tuned over a rather wide range. A reduction in the reflectance of the system by nanocoatings was also observed in earlier studies [4, 19].

5. Zero-reflection condition

It is of interest to derive conditions for complete suppression of reflection from the substrate (zero-reflection conditions). Setting the reflected wave amplitude in (15) equal to zero, we obtain the following relation between the parameters of the substrate and nanostructured layer:

$$\hat{G} = \frac{\hat{M}+\hat{P}+\left[\left(\hat{M}+\hat{P}\right)^2-\hat{C}_p^+(\boldsymbol{p})\hat{K}^2\right]^{1/2}}{\hat{K}}, \tag{16}$$

where

$$\hat{K} = 2\alpha_p\left\{\hat{C}_p^-(2\boldsymbol{\Delta})\exp[\mathrm{i}\boldsymbol{k}_0\boldsymbol{\Delta}+\mathrm{i}\boldsymbol{k}_{0\,\mathrm{refl}}(-\boldsymbol{\Delta}+\boldsymbol{p})]\right.$$
$$\left.-\hat{C}_p^-(2\boldsymbol{\Delta}-\boldsymbol{p})\exp(2\mathrm{i}\boldsymbol{k}_0\boldsymbol{\Delta})\right\};$$

$$\hat{M} = \exp[\mathrm{i}\boldsymbol{k}_0\boldsymbol{\Delta}+\mathrm{i}\boldsymbol{k}_{0\,\mathrm{refl}}(-\boldsymbol{\Delta}+\boldsymbol{p})]\left(1-\alpha_p\hat{A}_p\right);$$

$$\hat{P} = \alpha_p\left[\hat{C}_p^-(2\boldsymbol{\Delta}-\boldsymbol{p})-\hat{C}_p^+(\boldsymbol{p})\exp[2\mathrm{i}\boldsymbol{k}_0\boldsymbol{\Delta}\ )\right].$$

Note that the left-hand side of (16) refers to the substrate, whereas its right-hand side is fully determined by the geometry and material parameters of the monolayer of nanoparticles.

In some instances, Eqn (16) significantly simplifies. Consider a wave incident on a system along the normal to its surface. We neglect the contribution of decaying waves to the $\hat{C}_p^{\pm}$ tensors [see Eqn (A1) in the Appendix] because, as we showed previously [19], their amplitude is much smaller than that of the zeroth (undamped) harmonic in the range of geometric and material parameters examined. With these approximations, the zero-reflection condition (16) takes the form

$$\hat{G} = \mathrm{i}\,\frac{2\pi k_0}{|\boldsymbol{a}_1\times\boldsymbol{a}_2|}\,\frac{\alpha_p}{1-\alpha_p\hat{A}}\exp(-\mathrm{i}2k_0\Delta). \tag{17}$$

Figure 3 shows the reflection spectra of the system under consideration obtained by exact electrodynamic finite element computations [21]. The refractive index of the substrate was chosen so as to meet condition (17) at wavelengths of 550 (Fig. 3a) and 460 nm (Fig. 3b), and the parameters of the monolayer were set *a priori*. The material of the nanoparticles in Fig. 3a is a hypothetical medium with a refractive index $n = 1.8$, and that in Fig. 3b is silicon, with the known dispersion of its optical constants [27].

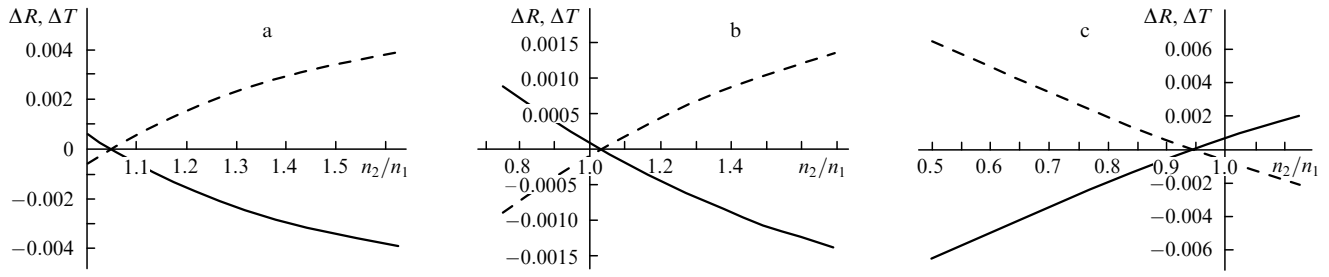

Figure 2. Deviations of the reflectance and transmittance of a system comprising a monolayer of spherical nanoparticles and a substrate from the Fresnel reflectance ($\Delta R = R - R_{\mathrm{F}}$, solid lines) and transmittance ($\Delta T = T - T_{\mathrm{F}}$, dashed lines) computed for normal incidence. Spheres of radius $a = 10$ nm have a refractive index $n = 1.5$ and are arranged in the form of a square lattice with a centre-to-centre distance of 30 nm. The monolayer is situated in a medium with an absolute refractive index $n_1 =$ (a) 1, (b) 1.33 and (c) 2.

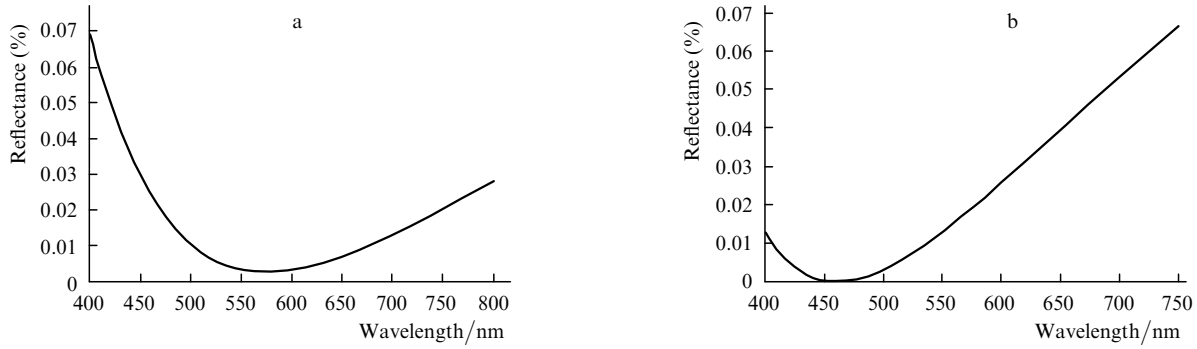

Figure 3. Reflection spectra of a system comprising a monolayer of spherical nanoparticles and a substrate: (a) $a = 15$ nm, $n = 1.8$, $n_2 = 1.03 + 0.11\mathrm{i}$; (b) $a = 20$ nm, $n = n(\omega)$ (silicon), $n_2 = 1.23 + 0.33\mathrm{i}$. A y-axis polarised wave is incident on the system along the normal to its surface ($\theta_I = 0$). The particles are arranged in the form of a square lattice with periods $|\boldsymbol{a}_{1,2}| = 3a$.

Note that in Fig. 3 the reflectance does not become zero at the minima (but the minimum reflectance is several hundred times lower than the reflectance of an uncoated substrate surface), and the minima are slightly shifted from the intended 550 and 460 nm, which is due to the discrepancy between the analytical solution (which was used to derive condition (17)) and the exact solution [19]. Therefore, in the case of large ($a \geqslant 20$ nm [19]) nanoparticles, the refractive index of the substrate found from (17) must also be slightly corrected using the exact solution. In this work, this was done by adjusting the corresponding parameter. In particular, the analytical refractive index of the substrate, n_2, in Fig. 3b is $1.1 + 0.36\mathrm{i}$, whereas the minimum in reflectance is reached at $1.23 + 0.33\mathrm{i}$. This is because condition (2) is not met, and the particles no longer behave as dipoles localised at their centre, so multipole terms in the expansion of the scattered field must be taken into account.

It should also be emphasised that reflection suppression is significant (by more than a factor of 10) in a rather broad wavelength range: from 460 to 800 nm in Fig. 3a and from 400 to 600 nm in Fig. 3b. Moreover, there is no absorption in the layer in Fig. 3a, and the average absorptance in the visible range in Fig. 3b is 0.13 %.

Reflection suppression by a nanostructured film on the surface of a medium offers considerable promise for producing antireflection coatings. Indeed, for some materials thin-film multilayer optical interference coatings are difficult to produce because of the dispersion of their refractive index or because one must use films with optical constants unattainable in bulk materials. The optical response of a coating composed of nanoparticles can be tuned by varying only the internal geometric parameters, which enables reflection suppression even in the above 'complicated' systems. For example, at a fixed refractive index of the substrate, changing the particle radius by 1 % shifts the minimum in reflectance by approximately 27 nm in Fig. 3a and 23 nm in Fig. 3b. Reducing the particle size shifts the minimum to shorter wavelengths, and vice versa. The lattice constant also influences the position of the zero-reflection region: with increasing lattice density, it shifts to longer wavelengths. If we fix not the optical constants of the substrate but the zero-reflection wavelength, the parameters of the monolayer at which condition (17) is met depend on the substrate, with the following relationship: the higher the reflectance of the substrate, the higher must be the effective absorbance of the metalayer (denser packing, larger particles or higher optical density of the particles). This conclusion is obvious because the wave generated by the monolayer then has a large amplitude and, accordingly, suppresses the stronger reflection from the substrate through destructive interference.

Another approach to substantially modifying the optical properties of a monolayer – substrate system is to change the geometry of the lattice of nanoparticles, e.g., to produce anisotropic metalayers with a non-square lattice or utilise nested sublattices. As an example, Fig. 4 shows the reflection spectrum of a medium with a coating in the form of a complex lattice consisting of two nested sublattices differing in particle size. Clearly, this approach allows the minimum-reflectance wavelength to be tuned over a considerable range.

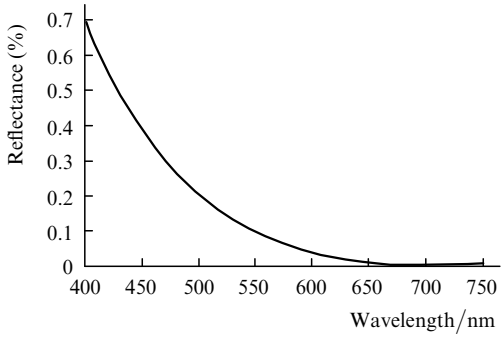

Figure 4. Reflection spectrum of two nested square lattices of 10- and 5-nm spheres on the surface of a semi-infinite medium. The period of the two sublattices is 30 nm, and the refractive indices of the spheres and substrate are $1.5 + 3\mathrm{i}$ and $0.96 + 0.22\mathrm{i}$, respectively. The parameters of the incident wave are the same as in Fig. 3.

6. Conclusions

We examined electrodynamic interaction between an ordered monolayer of spherical nanoparticles and a substrate. The results show that, in such systems, the fields reflected from the monolayer and the substrate surface may interfere both constructively and destructively, raising or reducing the reflectance of the entire system. We derived and analysed conditions for complete elimination of reflection from the substrate and identified the factors that influence the minimum-reflectance wavelength. Note that elimination of Fresnel reflection from the interface between

two media using a layer of carbon nanotubes or SiO_2 or TiO_2 nanorods has recently been demonstrated experimentally [28, 29].

One possible application of this effect is the engineering of antireflection coatings for existing artificial media with a refractive index close to unity [7]. According to the general theory of antireflection coatings [20], the refractive index of the antireflection film should then be closer to that of vacuum, so that no natural materials can be exploited for this purpose. The use of a loose structure with controlled optical characteristics, such as a monolayer of nanoparticles, makes it possible to substantially suppress or completely eliminate reflection from such materials, which in turn paves the way for engineering absolutely transparent materials.

Appendix

Lattice sums

To calculate the lattice sums (10) and (11), we take advantage of a procedure proposed by Ewald and successfully used in a number of studies [25, 26, 30]. Consider first the case where the point of observation is situated outside the layer. Given that the function describing the field of the dipoles is periodic, with a period equal to that of the lattice, it can be Fourier expanded in terms of reciprocal lattice vectors. Since the derivation of the expressions in question can be found in the aforementioned reports, we present only the result:

$$C_p(\boldsymbol{r}-\boldsymbol{r}_j)=-\sum_{p,q=-\infty}^{\infty}\frac{2\pi\mathrm{i}}{|\boldsymbol{a}_1\times\boldsymbol{a}_1|}[\boldsymbol{k}_{pq}(\boldsymbol{k}_{pq}\times\boldsymbol{n}_0)]\frac{\exp(\mathrm{i}\boldsymbol{k}_{pq}\boldsymbol{r})}{\kappa_{pq}}, \quad \text{(A1)}$$

where $\boldsymbol{n}_0=\boldsymbol{E}_I/|\boldsymbol{E}_I|$; $\kappa_{pq}=[k_0^2-(\boldsymbol{q}+\boldsymbol{g}_{pq}^{\mathrm{p}})^2]^{1/2}$; $\boldsymbol{g}_{pq}^{\mathrm{p}}=p\boldsymbol{g}_1+q\boldsymbol{g}_2$; and

$$\boldsymbol{k}_{pq}=\begin{cases}(\boldsymbol{q}+\boldsymbol{g}_{pq}^{\mathrm{p}},\kappa_{pq}), & \mathrm{z}>0,\\ (\boldsymbol{q}+\boldsymbol{g}_{pq}^{\mathrm{p}},-\kappa_{pq}), & \mathrm{z}<0.\end{cases} \quad \text{(A2)}$$

The reciprocal lattice vectors are given by

$$\boldsymbol{g}_1=2\pi\frac{\boldsymbol{a}_2\times\boldsymbol{n}}{|\boldsymbol{a}_1\times\boldsymbol{a}_2|}, \quad \boldsymbol{g}_2=2\pi\frac{\boldsymbol{n}\times\boldsymbol{a}_1}{|\boldsymbol{a}_1\times\boldsymbol{a}_2|}, \quad \text{(A3)}$$

where $\boldsymbol{a}_1=(\alpha,0,0)$ and $\boldsymbol{a}_2=(\beta,\gamma,0)$ are the translation vectors of minimal length in the real space lattice and the vector $\boldsymbol{n}=(0,0,1)$ is normal to the monolayer.

Equation (A1) is the expansion of the field of the monolayer into a plane harmonic wave ($p=q=0$) and a number of exponentially decaying waves, which emerge for $|\boldsymbol{q}+\boldsymbol{g}_{pq}|>k_0$, when the κ_{pq} coefficients are imaginary-valued.

To calculate the lattice sum (10) for a point of observation inside the metacoating, we use the Ewald method [25] to obtain the following relation at $z=0$:

$$\hat{A}_p=\hat{l}(\boldsymbol{k}_0)\boldsymbol{n}_0\exp(\mathrm{i}\boldsymbol{q}\boldsymbol{r}_j). \quad \text{(A4)}$$

The $\hat{l}$ tensor is symmetric, with l_{xz}, l_{yz}, l_{zx} and l_{zy} equal to zero, and has the form

$$l^{\mu\nu}(\boldsymbol{k}_0)=c^{\mu\nu}-\left[\frac{2}{3}\mathrm{i}k_0^3\mathrm{Erfc}\left(\frac{\mathrm{i}k_0}{2F}\right)+\frac{4F}{3\sqrt{\pi}}\left(k_0^2-F^2\right)\exp\left(\frac{k_0^2}{4F^2}\right)-\frac{2}{3}\mathrm{i}k_0^3\right]\delta^{\mu\nu}. \quad \text{(A5)}$$

This formula contains the complementary error function (Erfc), which rapidly approaches zero at large arguments, and

$$c^{\mu\nu}=\frac{\mathrm{i}\pi}{|\boldsymbol{a}_1\times\boldsymbol{a}_2|}\sum_{p,q}\left[\frac{k_0^2\delta^{\mu\nu}-k_{pq\nu}k_{pq\mu}}{\kappa_{pq}}\Delta_{pq}(1+\tau)+\eta\Sigma_{pq}\right]+\frac{1}{2}\sum_{n,m}\frac{\exp(\mathrm{i}\boldsymbol{k}_0\boldsymbol{a}_{nm})}{a_{nm}^3}\left\{\Gamma_{nm}^{(1)}\left[\delta^{\mu\nu}\Gamma_{nm}^{(2)}+\boldsymbol{a}_{nm}^{\mu}\boldsymbol{a}_{nm}^{\nu}\Gamma_{nm}^{(3)}\right]+\Gamma_{nm}^{(4)}\left[-\delta^{\mu\nu}a_{nm}+\boldsymbol{a}_{nm}^{\mu}\boldsymbol{a}_{nm}^{\nu}\Gamma_{nm}^{(5)}\right]+\mathrm{c.c}\right\}, \quad \text{(A6)}$$

where $\mu,\nu=x,y,z$; $\boldsymbol{a}_{nm}=n\boldsymbol{a}_1+m\boldsymbol{a}_2$; $a_{nm}=|\boldsymbol{a}_{nm}|$; n and m are integers; $\eta=\delta^{\mu z}\delta^{\nu z}$; $\tau=(-1)^{\delta^{\mu z}}(-1)^{\delta^{\nu z}}$;

$$\Delta_{pq}=\mathrm{Erfc}\left(-\frac{\mathrm{i}k_{pq}}{2F}\right); \quad \Sigma_{pq}=\frac{\mathrm{i}4F}{\sqrt{\pi}}\exp\left(\frac{k_{pq}^2}{4F^2}\right);$$

$$\Gamma_{nm}^{(1)}=\exp(-\mathrm{i}k_0a_{nm})\mathrm{Erfc}\left(a_{nm}F-\frac{\mathrm{i}k_0}{2F}\right); \quad \text{(A7)}$$

$$\Gamma_{nm}^{(2)}=-1-\mathrm{i}k_0a_{nm}+k_0^2a_{nm}^2; \quad \Gamma_{nm}^{(3)}=-k_0^2+\frac{3\mathrm{i}k_0}{a_{nm}}+\frac{3}{a_{nm}^2};$$

$$\Gamma_{nm}^{(4)}=\frac{2F}{\sqrt{\pi}}\exp\left(-F^2a_{nm}^2+\frac{k_0^2}{4F^2}\right);$$

$$\Gamma_{nm}^{(5)}=\frac{3}{a_{nm}}+2F^2a_{nm}; \quad F=\left(\frac{\pi}{|\boldsymbol{a}_1\times\boldsymbol{a}_2|}\right)^{1/2}.$$

The convergence of the sums in (A5) is determined by the F parameter, which has the dimensions of reciprocal length. This parameter has no physical meaning and is real-valued and positive. Substituting F into (A7), we can find the maximum values of m, n, p and q necessary for evaluating the lattice sums with a preset accuracy. Given that $\mathrm{Erfc}(x)=\exp(-x^2)/(x\sqrt{\pi})$ at large arguments, we obtain

$$\exp\left(-\frac{\pi a_{nm}^2}{|\boldsymbol{a}_1\times\boldsymbol{a}_2|}\right)\approx\xi, \quad \text{(A8)}$$

where ξ is a small parameter that characterises the computation accuracy. Exact computations for a square lattice show that varying m, n, p and q from -2 to 2 ensures a relative accuracy in the lattice sums of about 10^{-4} %, which agrees well with estimate (A8).

References

1. Shalaev V.M., Wenshan Cai, Uday K. Chettiar, et al. *Opt. Lett.*, **30**, 3356 (2005).
2. Smith D.R., Pendry J.B. *J. Opt. Soc. Am. B*, **23**, 391 (2006).
3. Agranovich V.M., Shen Y.R., Baughman R.H., et al. *Phys. Rev. B*, **69**, 165112 (2004).
4. Gadomskii O.N., Shalin A.S. *Zh. Eksp. Teor. Fiz.*, **132**, 870 (2007).
5. Grigorenko A.N., Geim A.K., Gleeson H.F., et al. *Nature*, **438**, 335 (2005).

6. Zhang S., Fan W., Panoiu N.C., et al. *Phys. Rev. Lett.*, **95**, 137404 (2005).
7. Xi J.-Q., Kim Jong Kyu, Schubert E.F., Ye Dexian, Lu T.-M., Lin Shawn-Yu, Juneja Jasbir S. *Opt. Lett.*, **31**, 601 (2006).
8. Mishchenko M.I., Travis L.D., Lacis A.A. *Scattering, Absorption and Emission of Light by Small Particles* (Cambridge: Cambridge University Press, 2002).
9. Haarmans M.T., Bedeaux D. *Thin Sol. Films*, **224**, 117 (1993).
10. Mie G. *Ann. Phys.*, **25**, 377 (1908).
11. Shalin A.S. *Zh. Prikl. Spektrosk.*, **73**, 641 (2006).
12. Shalin A.S. *Izv. Vyssh. Uchebn. Zaved., Ser. Fiz.*, **49**, 3 (2006).
13. Arfken G.B., Weber H.J. *Mathematical Methods for Physicists* (New York: Acad. Press, 1995).
14. Liu Z., Boltasseva A., Pedersen R.H., Bakker R., Kildishev A.V., Drachev V.P., Shalaev V.M. *Metamaterials*, **2**, 45 (2008).
15. Taflove A., Hagness S.C. *Computational Electrodynamics: The Finite-difference Time-Domain Method* (Boston: Artech House, 2000).
16. Prather D.W., Shi S. *J. Opt. Soc. Am. A*, **16**, 1131 (1999).
17. Chaumet P.C., Rahmani A., Bryant G.W. *Phys. Rev. B*, **67**, 165404 (2003).
18. Curry A., Nusz G., Chilkoti A., Wax A. *Opt. Express*, **13**, 2668 (2005).
19. Shalin A.S., Moiseev S.G. *Opt. Spektrosk.*, **106**, 1029 (2009).
20. Born M., Wolf E. *Principles of Optics* (Oxford: Pergamon, 1969; Moscow: Nauka, 1973).
21. COMSOL Multiphysics 3.4, COMSOL AB, Stockholm, Sweden; http://www.comsol.com/products/multiphysics/.
22. Bohren C.F., Huffman, D.R. *Absorption and Scattering of Light by Small Particles* (New York: Wiley, 1983; Moscow: Mir, 1986).
23. Evlyukhin A.B., Bozhevolnyi S.I. *Phys. Rev. B*, **71**, 134304 (2005).
24. Gadomskii O.N., Shalin A.S. *Fiz. Met. Metalloved.*, **101**, 462 (2006).
25. Poppe G.P.M., Wijers C.M.J., Silfhout A. *Phys. Rev. B*, **44**, 7917 (1991).
26. Wijers C.M.J., Poppe G.P.M. *Phys. Rev. B*, **46**, 7605 (1992).
27. Palik E.D. *Handbook of Optical Constants of Solids* (New York: Acad. Press, 1985).
28. Garcia-Vidal F.J. *Nature Photon.*, **2**, 215 (2008).
29. Xi J.-Q., Schubert M.F., Kim Jong Kyu, et al. *Nature Photon.*, **1**, 176 (2007).
30. Sukhov S.V., Krutitsky K.V. *Phys. Rev. B*, **65**, 115407 (2002).